

Electronic and structural characterization of LiF tunnel barriers in organic spin-valve structures

Greg Szulczewski,^{1,a)} Jonathan Brauer,¹ Edward Ellingsworth,¹ Justin Kreil,¹ Hailemariam Ambaye,² and Valeria Lauter²

¹Department of Chemistry, The University of Alabama, Tuscaloosa, Alabama 35487, USA

²Neutron Scattering Science Division, Oak Ridge National Laboratory, Oak Ridge, Tennessee 37831-6475, USA

(Presented 16 November 2010; received 24 September 2010; accepted 17 December 2010; published online 8 April 2011)

The electronic, magnetic, and structural properties of Ni₈₀Fe₂₀ and Co electrodes at LiF and aluminum tris(8-hydroxyquinoline), or Alq₃, interfaces were investigated with photoemission spectroscopy and polarized neutron reflectivity measurements. When LiF was deposited onto Ni₈₀Fe₂₀ films and Co was deposited onto thin LiF layers, the work function of both metals decreased. Polarized neutron reflectivity measurements were used to probe the buried interfaces of multilayers resembling a spin-valve structure. The results indicate that LiF is an effective barrier layer to block diffusion of Co into the Alq₃ film. X-ray absorption spectra at the fluorine *K* edge indicate that no chemical reactions occur between Co and LiF. Despite these positive effects derived from the LiF tunnel barriers, there was no magnetoresistance in spin valves when the Alq₃ layer was greater than 50 nm. © 2011 American Institute of Physics. [doi:10.1063/1.3562255]

Schmidt *et al.* were the first to point out the “conductivity mismatch” problem that limits efficient injection of spin-polarized electrons from ferromagnetic transition metals into inorganic semiconductors.¹ Rasha, followed by Fert and Jaffrès, suggested that the problem could be surmounted by inserting a tunnel barrier between the two materials.^{2,3} Recently, the use of tunnel barriers in organic spin valves has been actively pursued to improve the injection efficiency of spin-polarized electrons from ferromagnetic electrodes into organic semiconductor layers. For example, Dediu and co-workers have shown that inserting an Al₂O₃ buffer layer on top of Alq₃ films before deposition of a Co film reduced the reaction of Co with Alq₃ and improved the magnetic switching of the Co layer.^{4,5} Furthermore, Drew *et al.* reported that spin-polarized electrons from a Ni₈₀Fe₂₀ electrode can be injected across a 1 nm LiF barrier into Alq₃ based spin valves.⁶ In related work Liu *et al.* used polarized neutron reflectivity to characterize Co films deposited onto Alq₃ films⁷ and found that rougher interfaces yielded lower magnetoresistance values in spin valves. Collectively these results suggest that inorganic barriers should improve the quality of the interface between ferromagnetic metals and Alq₃ and result in higher magnetoresistance (MR) values.

Lithium fluoride was chosen as the tunnel barrier since it has been widely used in organic light emitting diodes since Hung *et al.* showed it can significantly lower the electron injection energy barrier between Alq₃ and metallic cathodes.⁸ There are ample spectroscopic data to suggest that LiF does not dissociate when deposited directly onto Alq₃.^{9–16} The initial growth of LiF on Alq₃ occurs via island formation followed by a pseudolayer-by-layer growth mechanism.^{17–20} Theoretical considerations suggest that insertion of a tunnel

barrier between a ferromagnetic metal and organic semiconductor should improve spin-polarized electron injection efficiency.²¹ Despite the perceived importance of the tunnel barriers in organic spin valves, only a few experimental studies have examined how tunnel barriers between an organic semiconductor and a ferromagnetic electrode affect charge and spin injection in a device.^{22–26}

Thin films for polarized neutron reflectometry (PNR) experiments were deposited onto cleaned, precut pieces of oxidized Si(100) substrates by thermal evaporation. The growth rate for the Alq₃ films was ~ 1 Å/s while the LiF, Ni₈₀Fe₂₀, and Co films were deposited at ~ 0.1 Å/s. The PNR measurements were done at the Spallation Neutron Source at Oak Ridge National Lab using the Magnetism Reflectometer on beamline 4A.²⁷ The neutron wavelength band is from 2 to 5 Å and the polarization of the neutron beam is $\sim 98\%$. Magnetic and nuclear scattering is separated using neutrons polarized parallel (“+” state) or antiparallel (“–” state) to the external field.

Ultraviolet photoelectron spectra of LiF deposited onto Ni₈₀Fe₂₀ films and LiF deposited onto Co films were measured in an ultrahigh vacuum chamber attached directly to a high vacuum deposition chamber. In the deposition chamber the metals were deposited by electron beam bombardment. The Alq₃ and LiF were deposited from homemade Knudsen type cells using alumina crucibles. Unfiltered, unpolarized He(I) radiation at 21.2 eV was produced from a differentially pumped discharge lamp (Specs, model UVS 20-A). The emitted photoelectrons were detected perpendicular to the surface normal with a double-pass cylinder mirror analyzer (Physical Electronics, model 10-155) using a pass energy of 10 eV. In order to measure work function changes the sample was held at a -4 V dc bias to observe the shift in the secondary-electron cut-off region. X-ray absorption spectra (XAS) were measured at the University of Wisconsin–Madison Synchrotron Radiation Center by measuring the sample drain current.

^{a)}Author to whom correspondence should be addressed. Electronic mail: gjs@bama.ua.edu. FAX: (205) 348-9104.

The experimental PNR data (symbols) and fit (solid lines) are shown in the top panel of Fig. 1 for the sample $\text{Ni}_{80}\text{Fe}_{20}$ (10 nm)/LiF(2 nm)/ Alq_3 (100 nm)/LiF(2 nm)/Co(4 nm)/Al(10 nm) grown onto a Si(100) substrate, where the values for the layer thickness in parentheses represent the nominal QCM values. The multilayer was cooled to 10 K in an external magnetic field of 0.2 T applied in plane of the sample surface to align the magnetization directions of the $\text{Ni}_{80}\text{Fe}_{20}$ and Co electrodes. Figure 1 also shows the nuclear scattering length density (middle panel) and the magnetic scattering length density (bottom panel) profiles extracted from the fit to the data. The layer thicknesses obtained from the fit are close to the QCM

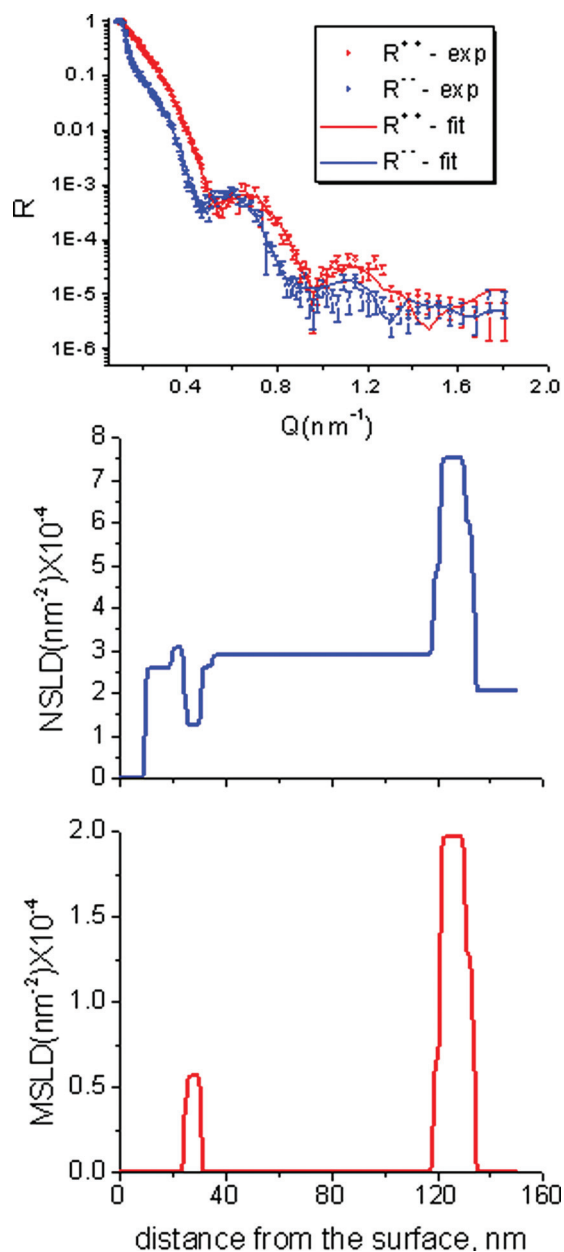


FIG. 1. (Color online) (Top) Specular neutron reflectivity data measured at 10 K in a 0.2 T in-plane magnetic field for the sample: $\text{Ni}_{80}\text{Fe}_{20}$ (10 nm)/LiF(2 nm)/ Alq_3 (100 nm)/LiF(2 nm)/Co(4 nm)/Al(10 nm)/Si(100) where the film thickness in parentheses represents the QCM value. (Middle) Nuclear scattering length density profile as a function from the distance to the surface obtained from the fitting procedure. (Bottom) Magnetic scattering length density profile obtained from the fitting procedure.

values. An important conclusion from the fit is that interfaces are rather “abrupt” (with the interfacial regions less than 0.5 nm), which suggests minimal intermixing. This is consistent with atomic force microscopy images (not shown) taken after deposition of LiF and Co onto Alq_3 films. More important, the PNR results give high resolution in-depth ($<0.5\text{nm}$) information averaged over the *whole lateral size* of the sample (14×7 mm) and prove that the buried interfaces in the devices remain abrupt after subsequent deposition of each layer *in situ* and that no detectable diffusion across the interfaces occurs.

Figure 2 shows ultraviolet photoelectron spectra for 0.5, 1, and 2 nm LiF films grown onto a 5 nm $\text{Ni}_{80}\text{Fe}_{20}$ film. There is one predominant peak with binding energy initially near 8.5 eV, which is assigned to the F(2p) derived state of the LiF valence band.²⁸ The binding energy of this peak gradually increases with increasing LiF thickness. A similar trend was reported for LiF deposition of Al and Pt surfaces.²⁹ In the spectra of the 2 nm LiF film there is a lower binding energy shoulder between 6 and 7 eV that has been attributed to possible defect states.^{14,29} After deposition of a 2 nm LiF layer on the $\text{Ni}_{80}\text{Fe}_{20}$ film the work function decreased by about 1.4 eV and the *d* band of the $\text{Ni}_{80}\text{Fe}_{20}$ layer is almost completely attenuated. The decrease in the work function is consistent with both experimental and theoretical studies. Pong and Paudyal measured the change in the photoemission threshold for thin (less than ~ 2 nm) LiF layers deposited on clean thin films of Mg, Al, Cr, Ag, Pt, and Au.³⁰ They found that LiF deposition systematically lowered the threshold for photoemission, i.e., decreased the work function. There is also theoretical evidence that predicts LiF adsorption on metals lowers the work function. Prada *et al.* used density functional theory to calculate the work function change for three monolayers of LiF adsorbed on the (100) plane of Al, Pd, Pt, Mo, Ag, and Au surfaces.³¹ The work function of each metal decreased upon LiF adsorption. By analyzing the projected density of states for each LiF/metal interface, Prada *et al.* concluded that very little charge transfer occurs between LiF and the metals. Instead the reduction in the work function is best described as electrostatic compression of the metal wave function. Figure 3 shows ultraviolet photoelectron spectra for a 20 nm Alq_3 film, a 1 nm LiF layer deposited on Alq_3 , and 0.2, 0.5, 1, and 4 nm

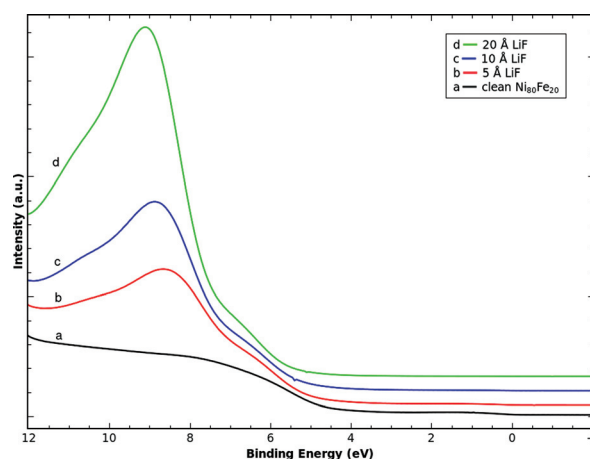


FIG. 2. (Color online) Ultraviolet photoelectron spectra for (b) 0.5-, (c) 1-, and (d) 2-nm-thick LiF films deposited onto a 5 nm $\text{Ni}_{80}\text{Fe}_{20}$ film shown in (a).

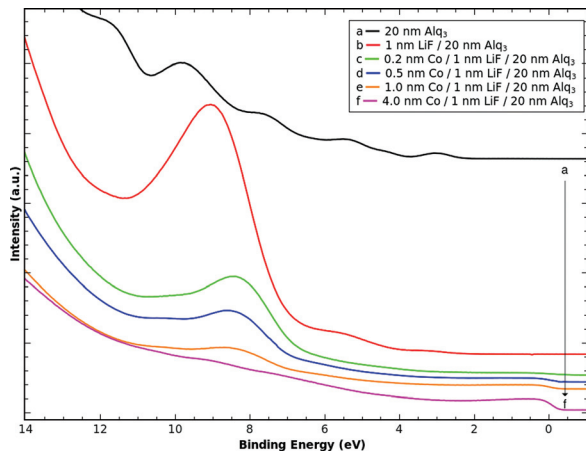


FIG. 3. (Color online) Ultraviolet photoelectron spectra for (a) 20 nm Alq₃ film and (b) 1 nm LiF film on Alq₃. The spectra labeled (c), (d), (e), and (f) show 0.2, 0.5, 1 and 4 nm Co films subsequently deposited onto the 1 nm LiF/20 nm Alq₃ bilayer.

films of Co deposited onto the LiF/Alq₃ bilayer. The Co work function increases from 4.0 to 5.0 eV when the film thickness is increased from 0.2 to 4 nm Co. In general, the ultraviolet photoelectron spectra shown in Figs. 2 and 3 agree with the widely accepted conclusion that LiF layers sandwiched between metal and Alq₃ films lowers the energy barrier between the Fermi energy of the metal and lowest unoccupied molecular orbital in Alq₃.^{9,14}

Figure 4 shows XAS spectra of the fluorine *K* edge for a 2 nm LiF film deposited onto a 20 nm Alq₃ film and a 3 nm Co film deposited onto a 2 nm LiF/20 nm Alq₃ film. Both LiF films have three peaks above the absorption edge near 696, 699, and 704 eV. The line shape of the spectra are similar to one published for a LiF single crystal.³² Based on the similar line shape of the absorption spectra we conclude that Co does not react with LiF. This assertion is further supported by a simple thermodynamic calculation that predicts the Gibbs free energy change for the reaction of Co with LiF to produce Li and CoF₂ is positive, so the reaction is not spontaneous.³³

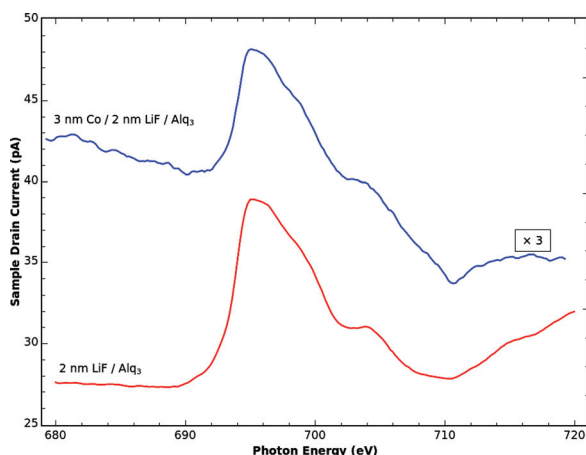


FIG. 4. (Color online) X-ray absorption spectra in the fluorine *K*-edge region for a 2 nm LiF layer grown on a 20 nm Alq₃ film (bottom) and a 3 nm Co layer deposited onto the 2 nm LiF/20 nm Alq₃ film (top).

Despite the positive impact of LiF on Ni₈₀Fe₂₀ and Co interfaces, room temperature magnetoresistance was not observed in organic spin valves when the Alq₃ layer was thicker than 50 nm. However a spin valve using La_{0.67}Sr_{0.33}MnO₃ as the bottom electrode and a single 2 nm LiF tunnel barrier on a 10 nm tetraphenylporphyrin layer with a top Co electrode did show a negative magnetoresistance of ~20% at 11 K.³⁴

In summary, deposition of LiF on Ni₈₀Fe₂₀ lowers the work function by 1.4 eV, which results in the reduction of the barrier to electron injection into Alq₃ films. The PNR and XAS measurements suggest that the LiF buffer layer prevents the reaction and diffusion of Co into the Alq₃ film. The lack of MR suggests that paramagnetic defects in the LiF tunnel barriers may increase spin-flip scattering, which reduces the spin polarization.

The authors thank MINT Center at the University of Alabama and the Department of Energy (Award No. DE-FG02-08ER46499) for partial support of this work. The research at the Oak Ridge National Laboratory Spallation Neutron Source was made possible through Award No. IPTS-2442, which was sponsored by the Scientific Users Facility Division through the U.S. Department of Energy. The work based on research at the University of Wisconsin–Madison Synchrotron Radiation Center was supported by the National Science Foundation under Award No. DMR-0537588.

- ¹G. Schmidt, D. Ferrand, and L. W. Molenkamp, *Phys. Rev. B* **62**, R4790 (2000).
- ²E. I. Rashba, *Phys. Rev. B* **62**, R16267 (2000).
- ³A. Fert and H. Jaffrès, *Phys. Rev. B* **64**, 184420 (2001).
- ⁴Y. Q. Zhan *et al.*, *Appl. Phys. Lett.* **94**, 053301 (2009).
- ⁵F. Borgatti *et al.*, *Appl. Phys. Lett.* **96**, 043306 (2010).
- ⁶A. J. Drew *et al.*, *Nature Mater.* **8**, 109 (2008).
- ⁷Y. Liu *et al.*, *Phys. Rev. B* **79**, 075312 (2009).
- ⁸L. S. Hung, C. W. Tang, and M. G. Mason, *Appl. Phys. Lett.* **70**, 152 (1997).
- ⁹T. Mori *et al.*, *Appl. Phys. Lett.* **73**, 2763 (1998).
- ¹⁰D. Yoshimura *et al.*, *Synth. Met.* **102**, 1145 (1999).
- ¹¹Q. Toan Le *et al.*, *J. Appl. Phys.* **87**, 375 (2000).
- ¹²M. G. Mason *et al.*, *J. Appl. Phys.* **89**, 2756 (2001).
- ¹³P. He *et al.*, *Appl. Phys. Lett.* **82**, 3218 (2003).
- ¹⁴T. Yokoyama *et al.*, *Jpn. J. Appl. Phys.* **42**, 3666 (2003).
- ¹⁵C.-I. Wu, G.-R. Lee, and T.-W. Pi, *Appl. Phys. Lett.* **87**, 212108 (2005).
- ¹⁶S. K. M. Jönsson, W. R. Salaneck, and M. Fahlman, *J. Appl. Phys.* **98**, 014901 (2005).
- ¹⁷Y. J. Lee *et al.*, *Ultramicroscopy* **108**, 1315 (2008).
- ¹⁸M. G. Helander *et al.*, *J. Appl. Phys.* **104**, 094510 (2008).
- ¹⁹Z. T. Xie *et al.*, *Appl. Phys. Lett.* **94**, 063302 (2009).
- ²⁰J. H. Lee, D. W. Moon, and Y. Yi, *Org. Electron.* **11**, 164 (2010).
- ²¹M. Yunus, P. P. Ruden, and D. L. Smith, *J. Appl. Phys.* **103**, 103714 (2008).
- ²²T. S. Santos *et al.*, *Phys. Rev. Lett.* **98**, 016601 (2007).
- ²³J. H. Shim *et al.*, *Phys. Rev. Lett.* **100**, 226603 (2008).
- ²⁴K. V. Raman *et al.*, *Phys. Rev. B* **80**, 195212 (2009).
- ²⁵J. J. H. M. Schoonus *et al.*, *Phys. Rev. Lett.* **103**, 146601 (2009).
- ²⁶G. Szulczewski *et al.*, *Appl. Phys. Lett.* **95**, 202506 (2009).
- ²⁷<http://neutrons.ornl.gov/instruments/SNS/MR/userinfo.shtml>.
- ²⁸E. L. Shirley *et al.*, *Phys. Rev. B* **53**, 10296 (1996).
- ²⁹R. Schlaf *et al.*, *J. Appl. Phys.* **84**, 6729 (1998).
- ³⁰W. Pong and D. Paudyal, *Phys. Rev. B* **23**, 3085 (1981).
- ³¹S. Prada, U. Martinez, and G. Pacchioni, *Phys. Rev. B* **78**, 235423 (2008).
- ³²E. Hudson *et al.*, *Phys. Rev. B* **49**, 3701 (1994).
- ³³Using the standard enthalpy and entropy values for Co, Li, LiF, and CoF₂ from the NIST Chemistry WebBook (available at <http://webbook.nist.gov>) we calculated the Gibbs free energy change to be a positive value between 300 and 1500 K.
- ³⁴W. Xu, Ph.D. dissertation, The University of Alabama, 2008.